New Insight into the Electric Field Distribution in OLEDs

D. Berner [+], E. Tutiš[°*+], L. Zuppiroli[°]

[+] CFG microelectronic, CH-1110 Morges, Switzerland

[°] LOMM/IMX, Ecole Polytechnique Fédérale CH-1015 Lausanne, Switzerland

* Institute of Physics, P.O.Box 304, HR-1000 Zagreb, Croatia

ABSTRACT

We report on an investigation of the electric field distribution inside organic light emitting devices (OLED's) using a combination of experimental study and numerical model simulations. Such an approach provides insight into the mechanisms responsible for the observed qualitative change in the electric field distribution as the applied voltage is increased. We found that the averaged electric field inside the hole transport layer is larger or equal to the average field in the emission layer over the entire current range.

INTRODUCTION

While the rapid and increasing interest in commercial applications of OLED's show that here is a huge economic potential behind this technology, OLED's are nevertheless far from being completely understood. Key industrial demands such as reliability and reproducibility make further improvements in the fundamental understanding of the basic processes necessary, especially an understanding of details like aging processes and light generation. For example, despite the fact that internal efficiency improvements are now reaching the absolute limit of 100% [1] the photon outcoupling rate of actually 20% is still not satisfactory [2], which depends among others on the layer thicknesses. However, the most critical key-parameter of OLED's is their lifetime, especially at high temperatures and for the red and blue colors. Some lifetime limiting factors like the glass transition temperature, anode surface quality, oxygen and water contaminations are already known [3-5], but the effect of space charges, field and recombination distribution are still open.

In this paper, we investigate by combining experimental results and numerical simulations the electric field distribution over the total organic layer thickness as a function of the applied voltage.

EXPERIMENTAL DETAILS

In order to investigate the influence of the hole transport and the emission layer thicknesses on the electric field distribution, we fabricated a variable-thickness 4 x 4 matrix device with the general composition ITO/CuPc(10nm)/α-NPD/Alq_3/LiF(0.8nm)/Al. The ITO (indium-tin-oxide) electrode, deposited on a glass substrate (30 $\Omega/\square$, Applied Film Corp.), was covered by a 10 nm thick CuPc (copper phthalocyanine) layer. These substrates were first cleaned in ethanol, acetone and soap ultrasonic bathes before evaporating a stepped gradient layer of 30, 40, 50 and 60 nm of α-NPD (N,N'-diphenyl -N,N'-bis(1-naphthyl)-1,1'biphenyl-4,4''diamine), followed by a perpendicularly stepped gradient layer of 40, 60, 70 and 80 nm thick Alq_3 (Tris(8-hydroxyquinolato)aluminum). A 0.8 nm LiF layer was then deposited right after the Alq_3, at a rate of 0.2 Å/s. The Al line electrodes were deposited perpendicular to the ITO stripes at a rate of 10 Å/s. The active area of the diode segments was 9 mm^2.

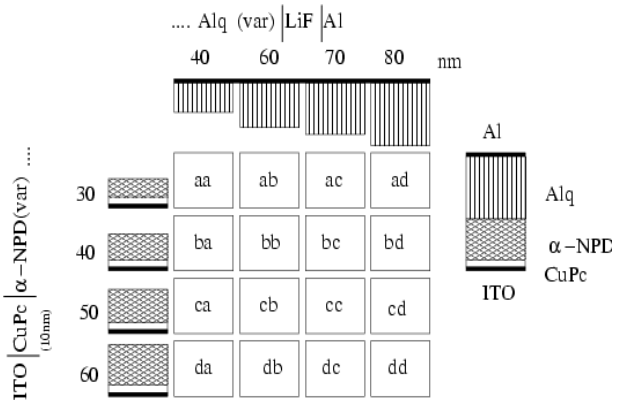

Figure 1: Labeling of the experimental measured I(V) lines

All layers were thermally evaporated at around $5*10^{-7}$ mbar and during the same fabrication process. All organics were purified by gradient sublimation and evaporated at a rate of 1.0 Å/s. The current versus voltage I(V) characteristics of each device were measured in a nitrogen atmosphere glove box by means of a LabView controlled Keithley 236 measuring unit. After, the resistivity contribution of the ITO-line on the I(V) curves was subtracted. This is an important procedure for a matrix geometry and for high performance diodes (low impedance)!

RESULTS AND DISCUSSION

We have found that the voltage dependence of the diode can be divided into four regions (Fig.: 2). The first region ① is characterized by the transport of a single type of carrier. In the second region ②, we observe a steep increase of the diode current corresponding to two-carrier injection, which leads to light generation. The 16 I(V) curves group in one way in this region, as we will discuss below. A different type of ordering among I(V) lines characterizes the third region ③. In this region ④, the high voltage range, the I(V) curves become less steep, and the ordering disappears. In this article, we will focus mainly on the ordered ranges ② and ③.

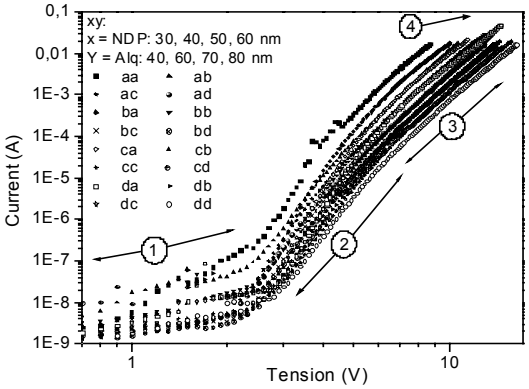

Figure 2: Current vs. voltage for the 16 matrix elements is presented. The numbers in the figure mark the different behavior ranges. At first sight, the ensemble of IV curves looks structureless and disordered, but as discussed in the text, a different kind of ordering appears in ranges ② and ③.

Figure 3 shows the current vs. the electric field (E-field) for the IV-range ②. Here the E-field denotes the averaged field across all organic layers. Looking in detail, we can see that the curves marked by ●, ⊗, ⊕, ○, representing the four different α-NPD layers thicknesses (30, 40, 50, 60 nm) lie on the same line for constant Alq_3 layer thickness of 80 nm. Looking at the full symbols ■, ▲, ★, ● (40, 60, 70, 80 nm of Alq_3 with 60 nm of α-NPD), we see that the average electric field across the whole device increases as the thickness of the Alq_3 layer decreases, which indicates a non-constant E-field behavior.

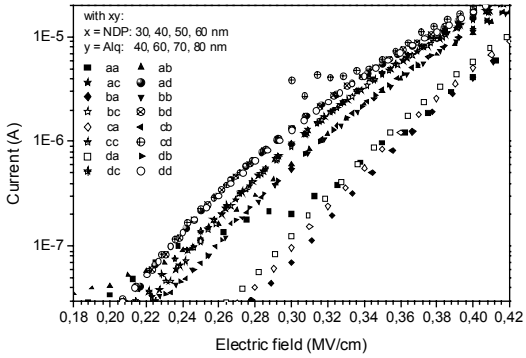

Figure 3: Expansion of current vs. E-field of range ②. It is clearly seen, that all IV curves of different α-NPD and constant Alq_3 layer thicknesses lie on the same line in this range, except the slightly variation for the thin 40 nm Alq_3 series.

Another type of rearrangement is seen in the Fig. 4, which presents the I(V) curves of range ③. Here, the curves corresponding to devices with the same *total* thickness lie on the same line, independent of device composition. This behavior indicates that, the average electric field in α-NPD and Alq_3 are of the same value in this range.

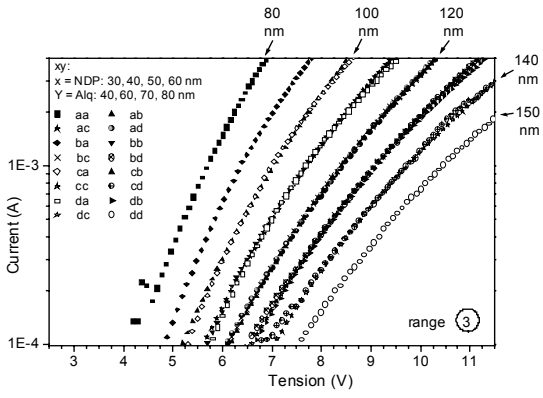

Figure 4: Extension of part ③ of Figure 2 is shown.

From these experimental curves, we have calculated the average electric fields of the α-NPD and Alq_3 layers. We have used therefore 8 sets of 4 I(V) lines corresponding to a fixed layer thickness of one layer type and the 4 corresponding layer thicknesses of the other material. For each of these 8 sets, a linear fit to the voltages for a constant current was made over the 4 different thicknesses, leading to an averaged electric field inside the varied layer. This was done for different current values. A representative E-field pair of this surprising result is presented in Figure 5.

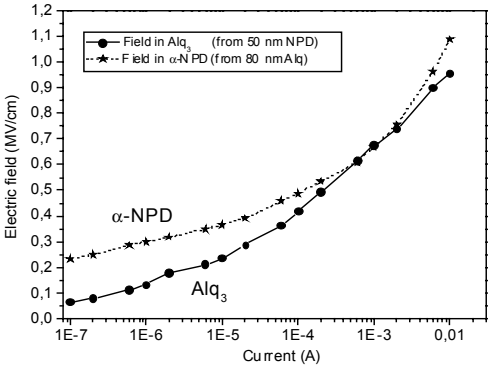

Figure 5: Averaged electric field of the α-NPD and Alq_3 layers inside our device, calculated from the experimental results. For the other thickness values qualitatively similar results are obtained.

We now discuss the particular situation of our device. Figure 5 shows that the average electric field in α-NPD is larger or equal to the average field in Alq_3 over the entire current range. In the current range above $1*10^{-4}$A these fields are relatively close in value. As it will be shown in more detail in the next section this result is caused by the rather balanced electron and hole injection at respective electrodes.

It should be noted here that, even for devices based on same or similar bilayer structure, this type of balance has not always observed by other authors. This discrepancy may be readily attributed to differences in the contact structure of the devices. For example, in Ref. [6], it was argued from the electroabsorption experiment that the field in Alq_3 is much bigger than in α-NPD. However, in that work no CuPc was used on the ITO side, and a Mg:Ag cathode was used instead of LiF/Al. On the other hand, it was argued in Ref [7] that CuPc might be used to balance the hole injection against electron injection at the Al/LiF/Alq_3 junction. At the same time, it was also argued there that CuPc reduces the hole injection from O_2-plasma treated ITO. Using a differently prepared CuPc on ITO sample, the opposite was recently observed by us [8]. This difference is not surprising, considering the effect that O_2-plasma treatment has on the workfunction of the ITO [9].

To simulate the behavior of our OLED devices a numerical device model was used [10-12]. The energy level data used in the numerical simulation were partially based on our cyclo-voltammetric measurements while the mobility parameters were taken from time of flight measurements published in the literature [13]. For a summary see Figure 6.

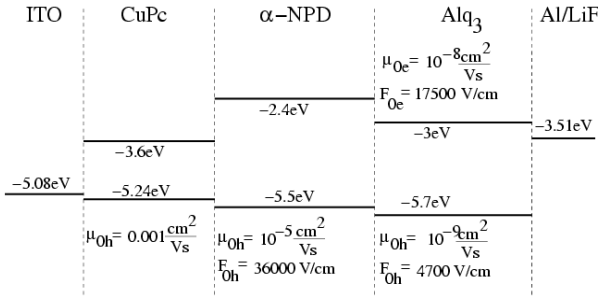

Figure 6: Energy levels and mobility data used in numerical model simulation.

In Figure 7 the carrier distribution in the 10nm/40 nm/60nm device is presented. Most of the charge accumulates in the region of the α-NPD/Alq_3 interface. Electrons are blocked at that interface and practically do not enter into the α-NPD layer. At the same time, holes do not only enter the Alq_3 layer but also dominate the charge density in the major part of the Alq_3 layer at low voltages. This leads to a non-negligible hole current leaking towards the cathode, which however, gradually disappears as voltage is increased. The increase of the electron density near the α-NPD/Alq_3 interface at higher current is responsible for the narrowing of the recombination zone. Most of the recombination is then confined to a few first monolayers near the α-NPD/Alq_3 interface. As the recombination increases, the *leak* hole current gradually diminishes with voltage and almost disappears.

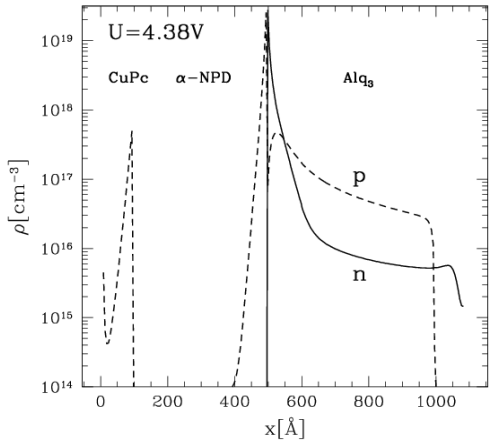

Figure 7: The charge distribution inside the device for 4.38V as obtained from the numerical simulation.

Also the region over which holes extend into Alq_3 shrinks towards the α-NPD/Alq_3 interface. Holes accumulate at the CuPc side of the CuPc/α-NPD interface too, reflecting the energy barrier present there.

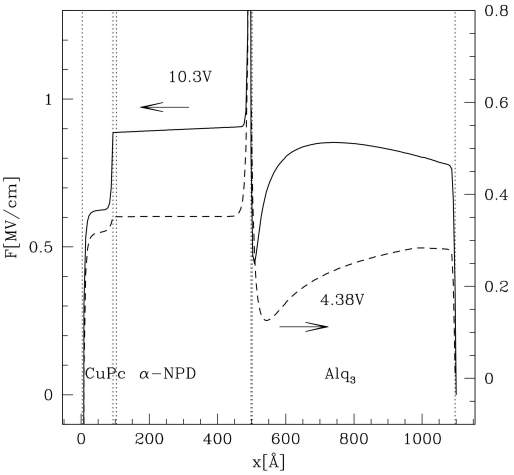

Figure 7: The electric field inside the device as obtained from the numerical simulation.

The effect of this may be also seen in Fig.: 7, which shows the variation of the electric field through the sample. This variation reflects the charge distribution in the device. The increase of the E-field in α-NPD with respect to its value in CuPc reflects the importance of the energetic barrier for holes at the CuPc/α-NPD interface. The big change in the electric field at the α-NPD/Alq_3 interface is due to the charge (mostly electrons) accumulated at that interface. In contrast, holes are responsible for the space charge effect inside the Alq_3-layer at low voltages. Again, this effect diminishes at high voltage when recombination becomes more effective and a smaller fraction of holes extends into the Alq_3.

In conclusion, our experimental analysis combined with numerical device modeling has proven to be a very useful tool for obtaining insight into the transport properties of OLED's. For the diode structure presented here, the analysis immediately suggests the following possible areas of improvement: a) making the CuPc/α-NPD interface more transparent to holes; b) preventing the holes from leaking to the cathode at low voltage; c) extending the recombination zone away from the first monolayer at the α-NPD/Alq_3 interface.

ACKNOWLEDGEMENTS

The authors are thankful to Dr. F. Nüesch and Dr. W. Leo for useful discussions. This work was supported in part by the SCOPES project number 7KRPJ065619.01 of the Swiss National Science Foundation.

REFERENCES

[1] C. Adachi, M. A. Baldo. E. Thompson, and S. Forrest, *J. Appl. Phys*., **90** (2001) 5048
[2] J. S. Kim, P. K. H. Ho, N. C. Greenham, R. H. Friend, J. Appl. Phys., **88** (2000) 1073
[3] J. S. Kim, R. H. Friend, F. Cacialli, Appl. Phys. Lett., **74** (1999) 3084
[4] Y. Sato, T. Ogata, J. Kido, Proc. SPIE **4105**, 134
[5] M. Schaer, F. Nüesch, D. Berner, W. Leo, L. Zuppiroli, *Adv. Funct. Mater.* **11** (2001) 116
[6] T. Yamada, F. Rohlfing, DC.Zou, T. Tsutsui, *Synth. Metals,* **111** (2000) 281
[7] E. W. Forsythe, M. A. Abkowitz, Y. Gao, *J.Phys.Chem. B*, **104** (2000) 3948
[8] B. Masenelli, D. Berner, M. N. Bussac, F. Nuesch, L. Zuppiroli, *Appl. Phys. Lett*. **79** (2001) 4438
[9] F. Nuesch, M. Carrara, M. Schaer, D.B. Romero, L. Zuppiroli, *Chemical Physics Lett.* **347** (2001) 311
[10] E. Tutis, M. N. Bussac, B. Masenelli, M. Carrard, L. Zuppiroli, *J. Appl. Phys*. **89** (2001) 430
[11] B. Masenelli, E. Tutis, M.N. Bussac, L. Zuppiroli, *Synthetic Metals* **122** (2001) 141
[12] B. Masenelli, E. Tutis, M. N. Bussac, L. Zuppiroli, *Synth. Metals* **121** (2001) 1513
[13] S. Naka, H. Okada, H. Onnagawa, Y. Yamaguchi, T. Tsutsui, *Synthetic Metals* **111-112** (2000) 331